Interpreting tracer breakthrough tailing from different forced-gradient tracer experiment configurations in fractured bedrock

Matthew W. Becker

Department of Geology, State University of New York at Buffalo, Buffalo, New York, USA

Allen M. Shapiro

Water Resources Division, U.S. Geological Survey, Reston, Virginia, USA

Received 16 January 2002; revised 31 October 2002; accepted 31 October 2002; published 30 January 2003.

[1] Conceptual and mathematical models are presented that explain tracer breakthrough tailing in the absence of significant matrix diffusion. Model predictions are compared to field results from radially convergent, weak-dipole, and push-pull tracer experiments conducted in a saturated crystalline bedrock. The models are based upon the assumption that flow is highly channelized, that the mass of tracer in a channel is proportional to the cube of the mean channel aperture, and the mean transport time in the channel is related to the square of the mean channel aperture. These models predict the consistent -2 straight line power law slope observed in breakthrough from radially convergent and weak-dipole tracer experiments and the variable straight line power law slope observed in push-pull tracer experiments with varying injection volumes. The power law breakthrough slope is predicted in the absence of matrix diffusion. A comparison of tracer experiments in which the flow field was reversed to those in which it was not indicates that the apparent dispersion in the breakthrough curve is partially reversible. We hypothesize that the observed breakthrough tailing is due to a combination of local hydrodynamic dispersion, which always increases in the direction of fluid velocity, and heterogeneous advection, which is partially reversed when the flow field is reversed. In spite of our attempt to account for heterogeneous advection using a multipath approach, a much smaller estimate of hydrodynamic dispersivity was obtained from push-pull experiments than from radially convergent or weak dipole experiments. These results suggest that although we can explain breakthrough tailing as an advective phenomenon, we cannot ignore the relationship between hydrodynamic dispersion and flow field geometry at this site. The design of the tracer experiment can severely impact the estimation of hydrodynamic dispersion and matrix diffusion in highly heterogeneous geologic media. *INDEX TERMS:* 1829 Hydrology: Groundwater hydrology; 1832 Hydrology: Groundwater transport; 5104 Physical Properties of Rocks: Fracture and flow; *KEYWORDS:* fractured rock, matrix diffusion, tracer tests, contaminant transport, advection dispersion, channeling

Citation: Becker, M. W., and A. M. Shapiro, Interpreting tracer breakthrough tailing from different forced-gradient tracer experiment configurations in fractured bedrock, *Water Resour. Res.*, *39*(1), 1024, doi:10.1029/2001WR001190, 2003.

1. Introduction

[2] A preponderance of evidence suggests that groundwater flows through only a fraction of the total porosity of un-weathered fractured bedrock, implying that "fast paths" may conduct contaminants very quickly to an exposure point [*Tsang and Neretnieks*, 1998]. The implied existence of fast paths has raised concerns about health risks from hazardous and nuclear-waste disposal in fractured rock [*Rasmuson and Neretnieks*, 1986; *National Research Council*, 1996]. Recently, research has targeted physical mechanisms that can mitigate fast-path transport by delaying mass en route [*Neretnieks*, 1980; *Haggerty and Gorelick*, 1994; *Ostensen*, 1998; *Haggerty et al.*, 2000]. The underlying concept of these mechanisms is that contaminant mass is exchanged between mobile water in high-velocity channels in fractures and relatively immobile water in inter-channel fluids, along fracture walls, and in the rock matrix. To predict contaminant transport in fractured rock, the critical next-step is to measure these mass-exchange processes in situ, and extract transport model parameters from the data.

[3] The most direct way to measure mass-exchange processes in the field is to perform an artificial tracer experiment. Typically, an artificial tracer experiment is performed by injecting a known mass of tracer into a forced or natural hydraulic gradient, and measuring the concentration of tracer as it arrives at one or more detection points. The history of concentration at a detection point is the breakthrough curve, from which transport parameters can be derived by matching the breakthrough data to an assumed transport model. Because physical

0043-1397/03/2001WR001190$09.00

mass-exchange is thought to take place relatively slowly with respect to advection, the breakthrough tail is usually the focus of attention when mass-exchange parameters are to be measured.

[4] A major complication associated with the measurement of mass-exchange processes, is that there are a number concurrent physical transport processes that affect the breakthrough curve (chemical processes are not addressed in this article). For purposes of discussion, these processes can be categorized as (1) hydrodynamic dispersion, (2) heterogeneous advection, and (3) matrix diffusion. In this article, we will use "hydrodynamic dispersion" to describe mass spreading related to local mixing and "heterogeneous advection" to describe mass spreading related to separation of advective pathways. We expect that hydrodynamic dispersion will increase spreading always in the direction of flow velocity, whereas heterogeneous advection may be reversed to some extent, when the flow field is reversed. For example, in the case of a slug of tracer injected into a formation, hydrodynamic dispersion and heterogeneous advection will increase spreading as the tracer moves away from the injection well. If the tracer is extracted by pumping the same well, mass spreading caused by heterogeneous advection will partially reversed, while hydrodynamic dispersion will continue to increase mass spreading. We assume therefore that hydrodynamic dispersion can be described by the advection-dispersion equation, while heterogeneous advection cannot. The term matrix diffusion is used here in the strict sense, that is, mass exchange between fractures and surrounding rock resulting from molecular diffusion.

[5] Hydrodynamic dispersion, heterogeneous advection, and matrix diffusion are not independent phenomena. Their relative influence on a tracer experiment can never be entirely distinguished. In a certain fractured formation, under a certain tracer experiment configuration, however, one or more of these three transport processes may dominate. For example, in a long-term tracer experiment conducted in a highly porous rock with permeable fractures, one might expect that matrix diffusion will control breakthrough tailing. In a short-term tracer experiment conducted in low-porosity rock with permeable fractures, one might expect advective processes will control breakthrough tailing. It is difficult to know a priori which of these transport processes will dominate a particular tracer experiment. If any one of these processes is to be measured, the other two must be sufficiently measured or otherwise constrained.

[6] Because of the inherent difficulty of independently measuring hydrodynamic dispersion, heterogeneous advection, and matrix diffusion, interpretation of a breakthrough curve usually requires fitting a multiparameter transport model to the data. At least three parameters are required to adequately fit a Fickian-based transport model to a breakthrough curve with significant tailing (representing advection, dispersion, mass exchange), so interpretations of tracer experiments are typically nonunique. One way to improve the uniqueness of a model is to stress the system, and see if the model still holds. With respect to hydrodynamic dispersion, for example, experiments can be performed at different transport velocities or over different distances [*Becker and Shapiro*, 2000]. With respect to matrix diffusion, experiments can be performed using tracers of different diffusivity [*Moench*, 1995; *Jardine et al.*, 1999; *Becker and Shapiro*, 2000; *Callahan et al.*, 2000]. With respect to heterogeneous advection, the critical parameter is the flow field. Consequently, stressing the system means conducting tracer experiments under different velocities and/or different hydraulic configurations. If a theoretical model can predict breakthrough tailing under different hydraulic conditions, it increases confidence that the interpretation is unique. Theoretical investigations [*Indelman and Dagan*, 1999] and laboratory "sandbox" experiments [*Chao et al.*, 2000] have shown, for example, that different estimates of dispersivity can be obtained from radial and uniform flow fields in porous media.

[7] Tracer tests employing a two-well (dipole) and radially converging design were compared at the Underground Research Laboratory (URL) in the Lac du Bonnet granite batholith, Pinawa, Manitoba [*Frost et al.*, 1995]. Although reversing the flow in the two-well tests produced similar breakthrough, the two-well tests and radially convergent tests produced markedly different results even though the same wells were used. Breakthrough from the convergent tests was much more disperse than that from the dipole tests, and in one radially convergent test, no tracer was recovered at all. Similarly, tracer tests conducted in a well pair at the Raymond Site in northern California produced good recovery under weak-dipole conditions [*Karasaki et al.*, 2000], but no recovery under strictly radially convergent conditions [*Becker*, 1996, pp. 52–53]. Weak-dipole (3.3% reinjection) experiments conducted at the C-wells complex at the Nevada Test Site produced a more rapid first arrival and peak arrival time than radially convergent tests between the same two wells [*Reimus et al.*, 1999]. By way of contrast, dipole and radially convergent tracer tests conducted between the same two wells in the metasediments and igneous suites of the Chalk River Site, Ontario, produced very similar results [*Raven et al.*, 1988]. A review of the literature therefore indicates that in fractured rock even a minor change in the induced flow field can have a major impact on tracer transport.

[8] In this article we consider forced-gradient tracer experiments conducted under various hydraulic configurations in a fractured crystalline bedrock. A theoretical model of transport is proposed that predicts tailing behavior in experiments conducted under (1) radially convergent, (2) weak-dipole, and (3) push-pull (injection/withdrawal) configurations. Previous experiments conducted in this formation produced identical breakthrough tails for tracers of varying diffusion rates. The independence of solute transport with respect to diffusion rate suggests that matrix diffusion does not significantly influence breakthrough tailing in short-term experiments [*Becker and Shapiro*, 2000]. The model offered herein consequently relies upon advective processes to explain breakthrough tailing. Specifically, breakthrough tailing is considered to be the result of channeling-like behavior in fractures, enhanced by the imposed artificial flow field.

2. Background

[9] Heterogeneous advective processes in fractured rock have often been referred to in the literature as "flow channeling" based upon the observation that water tends

to follow discrete pathways in tight fractures [*Tsang and Neretnieks*, 1998]. It is thought that channels develop as water under the influence of a hydraulic gradient attempts to find the path of least resistance. The path of least resistance is formed through the hydraulic connection of anomalously large apertures. Laboratory studies have shown that increased stress perpendicular to the plane of a fracture increases channeling [*Hakemi and Larsson*, 1996], and numerical studies have shown that channeling increases with the statistical variation in aperture [*Moreno and Tsang*, 1991; *Moreno and Tsang*, 1994]. Consequently, channeling is expected to be more dramatic in deep crystalline rock, where fractures are narrow and roughly surfaced, than in sedimentary rocks in which fractures form more smoothly along bedding planes. When aperture variation is large, the velocity distribution becomes even larger, and channels may become virtually independent, crossing only occasionally in the plane of a fracture [*Moreno and Tsang*, 1994]. For example, in a field tracer experiment in which concentration was monitored by drilling boreholes in the plane of a single fracture, it was estimated that water flowed primarily through only 20% of the fracture area [*Bourke*, 1987]. If one considers that in order for multiple fractures to be hydraulically connected, channels must "link up" at fracture junctures, it may be that channeling can have a more profound effect over larger transport distances [*Abelin et al.*, 1991; *Tsang et al.*, 1991]. *Parney and Smith* [1995] have suggested that transport paths in fractured media tend to lengthen as velocity increases. This implies that forced-gradient tracer experiments may produce more channeled flow than would exist under natural gradients.

[10] Although the use of channel models have supplanted earlier "parallel plate" models of fracture flow to some extent, the parallel plate model still dominates interpretation of flow and transport in a single fracture. Creeping flow between smooth parallel plates (Poiseuille flow) is expected to have a flow rate proportional to the cube of the distance between the plates (aperture) [*Tsang*, 1992]. A "local cubic law" is often applied to rough-walled fractures by assuming that the cubic law holds for a given aperture, even though the aperture varies throughout the fracture [*Neuzil and Tracy*, 1981; *Oron and Berkowitz*, 1998]. The relationship between the aperture obtained through frictional head loss (the "cubic law aperture" of *Tsang* [1992]) and the aperture obtained from tracer tests results (the "mass balance aperture" of *Tsang* [1992]) is the subject of some debate. Given that the volumetric flux of water (flow rate) and mass flux of solute must be related, it is logical to assume that tracer transport will be controlled by the cubic law in some respect. *Guimera and Carrera* [2000] argue that the cubic law and mass balance apertures should be proportional, with the proportionality constant related to the variance of the apertures within the flow field. The cubic law is therefore expected to control tracer breakthrough, even though comparison of resulting aperture estimations may be difficult among different field sites.

[11] *Haggerty et al.* [2000] reviewed models of mass-exchange processes as applied to fractured rock. Most of these models assume that mass exchange occurs between mobile and immobile water via molecular diffusion. Other researchers have suggested that micro-advective processes may also play a role [*Raven et al.*, 1988]. If a tracer moves along a streamline in a fracture, under creeping flow conditions, it is clear that molecular diffusion must play a role if any mass exchange between mobile and immobile water is to take place. Consequently, it is impossible to decouple the effects of advection and diffusion even at the microscopic scale. Some researchers have attempted to capture the complexity of matrix diffusion by allowing for multiple rates of mass transfer between mobile and immobile water [*Haggerty and Gorelick*, 1995; *Haggerty et al.*, 2000]. These mass transfer rates are intended to represent mass exchange via molecular diffusion. Because the exchange constants are not independently verifiable, however, they might actually represent a more complex process than simple molecular diffusion.

[12] Although research has tended to compartmentalize the study of breakthrough tailing in fractured rock, our view is that there is a broad continuum of transport processes that cause breakthrough tailing ranging from purely advective to purely diffusive phenomena (leaving chemical reactivity and buoyancy effects aside). An element that has been largely missing from this study is the influence of the imposed flow field upon the breakthrough tail. Because it is usually impractical to characterize the conductivity field of a fractured rock at multiple scales, interpretive models of tracer experiments have either assumed physical or stochastic homogeneity of the conductivity field. Resulting models therefore employ simplified flow geometries, based upon potential theory in a homogeneous medium. One might justifiably hypothesize the opposite; that it is the imposed flow field that causes breakthrough tailing. To test this hypothesis experimentally, tracer experiments must be interpreted under different forced gradient conditions. In this article, we hypothesize a conceptual transport model that illustrates how strongly heterogeneous flow fields can lead to breakthrough tailing phenomenon, under different hydraulic configurations. We compare tracer transport in experiments in which the flow field is reversed, and in which it is not, to highlight the different influences of (1) hydrodynamic dispersion, (2) heterogeneous advection, and (3) matrix diffusion.

3. Conceptual Model

[13] Consider a two-well tracer experiment in a single heterogeneous fracture in which tracer is continually being injected and extracted (a dipole or weak-dipole experiment). We assume a channel model of flow, such that two wells will be connected hydraulically by discrete, nonintersecting conduits of flow [*Shapiro and Nicholas*, 1989]. It is recognized that channels are not sealed from one another, but that large variations in velocity from one channel to the next make them behave relatively independently. At any given position in a channel along the path line, l, we apply the local cubic law [*Tsang*, 1992],

$$v(l) = -\frac{\gamma}{\mu}\frac{H^2}{12}\frac{dh}{dl}, \tag{1}$$

where v is the average fluid velocity (Darcy velocity), H is the fracture aperture at position, l, γ and μ are the specific weight and viscosity of the fluid, and dh/dl is the hydraulic gradient. Because we are assuming that channels are

hydraulically independent, flow rate in the channel will be constant throughout. Consequently,

$$Q = v(l)HW = -\frac{\gamma}{\mu}\frac{H^3 W}{12}\frac{dh}{dl}, \tag{2}$$

where Q is the flow rate in a channel and W is the width of the channel at any point, l, in the channel. The travel time of a conservative (nonreactive) tracer in this channel is of interest, so we define the mean travel time of a tracer along path, l, as [*Tsang*, 1992]

$$\tau = \int_{l_1}^{l_2} \frac{dl}{v(l)} = \int_{l_1}^{l_2} \frac{HWdl}{Q} = \frac{V}{Q}. \tag{3}$$

where V is the volume of an individual channel and Q is the flow rate through that channel. Equation 3 indicates that the mean travel time through the channel is simply the active fluid volume in the channel, divided by the flow rate. Equations 1–3 imply that tracer travel time along any channel will be related to the square of the mean fracture aperture, while the flow rate through the channel will be related to the cube of the mean fracture aperture.

[14] Tracer mass will enter the fractured formation as it travels; along individual channels. Assuming that the concentration of tracer, C_o, in the injection solution is homogeneous, the rate at which tracer mass enters a single channel is expected to be

$$\dot{m} = QC_o, \tag{4}$$

where $\dot{m}$ is the mass flux, and Q is the flow rate into the channel. Consequently, channels of aperture greater than the mean aperture are expected to contribute more tracer mass to the extraction well than channels of aperture less than the mean aperture. The total tracer mass in each channel is proportional to the cube of the mean aperture of the channel, and the rate of transport of that mass is proportional to the square of the mean aperture of the channel.

[15] Thus far only steady state two-well tracer experiments have been considered, but similar transport behavior would be expected from other tracer experiment designs. For example, under a radially convergent design, tracer is usually introduced as a finite volume of tracer-laden water or "slug" injected into the formation using a small overpressure. The typical procedure is to establish pseudo-steady flow to a single extraction well, and then inject the tracer slug into the flow field. During the short injection period, a hydraulic connection between the injection well and existing flow channels develops (Figure 1) and mass enters the formation at a rate proportional to the cube of the mean aperture of the channel. Because the volume of water injected is usually small and the injection duration short, channel geometry should remain approximately the same during and after injection. Thus even in the slug injection case the total tracer mass in each channel is proportional to the cube of the mean aperture of the channel and the rate of transport of that mass is proportional to the square of the mean aperture of the channel.

[16] In this conceptual model, each hydraulically separated channel will contribute tracer mass to the extraction well at a different flux rate. The total mass conveyed by a particular channel will be proportional to the cube of the mean aperture of the channel as indicated by equation 2 and equation 4. The mean arrival time of this mass will be proportional to the square of the mean aperture of the channel as given by equation (3). The measured breakthrough at the extraction well will therefore result from the sum of the transport through each channel, where each channel transport is offset by its particular mean arrival time.

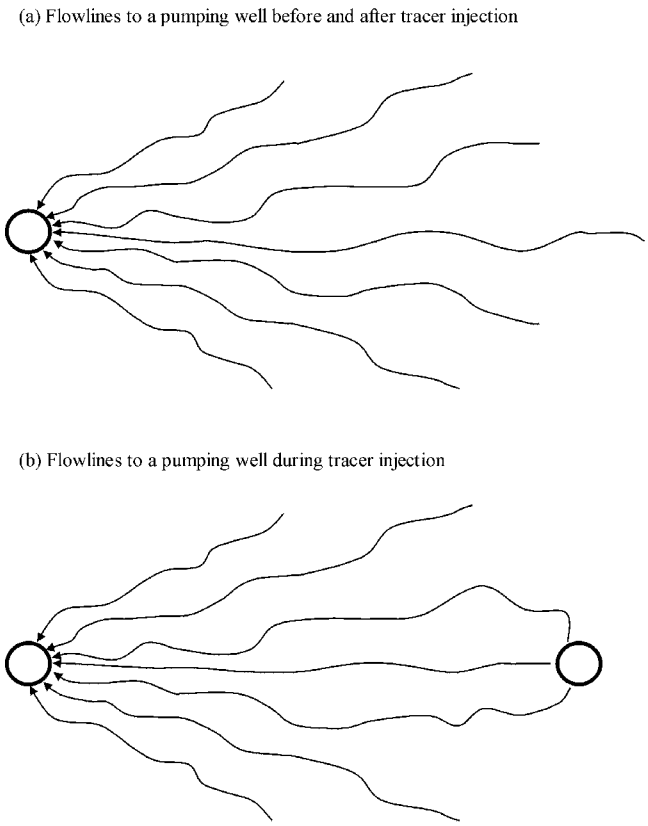

Figure 1. Schematic of flow lines to a pumping well. The flow field is temporarily disturbed during tracer injection, but is dominated by the pumping well.

[17] For simplicity, we will illustrate this conceptual model using a simple one-dimensional uniform flow transport equation. Radial solutions will be addressed later. Assuming transport in each channel is predicted by a uniform flow first passage time solution of the advection dispersion equation [*Becker and Charbeneau*, 2000], and an order-of-magnitude variation in mean aperture among channels, we predict breakthrough at the extraction well will resemble the curve depicted in Figure 2. Breakthrough from individual channels is shown in Figure 2 as dotted lines, and breakthrough from the sum of all channels is shown a solid line. In this example simulation, the Peclet number (Pe) is 15.

[18] It is important to note that the shape of the breakthrough from the sum of all channels is dependent upon the range of the apertures in the channels, but not the frequency distribution of apertures. This somewhat surprising result is a consequence of the coupled relationship between the mass entering the individual channel and the rate at which tracer travels along that channel. Both the amount of tracer mass

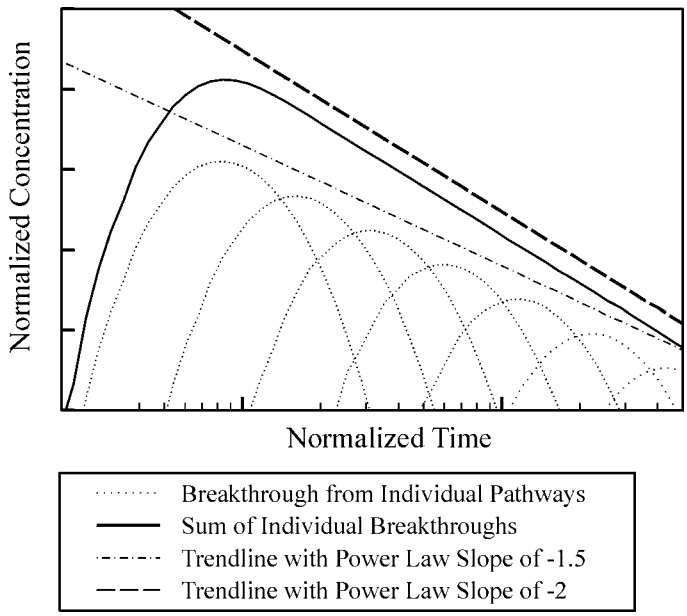

Figure 2. Hypothetical breakthrough at a well as a summation of mass transport along individual flow paths, shown on a log-log plot.

in a channel, and the velocity at which that mass moves, are related to the mean aperture of the channel. If there are a large number of channels with a given mean aperture, tracer mass will be divided among those channels equally. Thus the amount of tracer mass arriving at the mean transport time corresponding to that mean aperture is independent of the number of channels with that mean aperture. This independence was confirmed by comparing numerical predictions such as those shown in Figure 2, using various assumed distributions of channel mean apertures. The implication of this result is that information about the aperture distribution is lost due to biasing of the tracer distribution.

[19] Based upon simulations similar to that shown in Figure 2, only a very few channels are required to cause a smooth composite breakthrough when dispersion is significant (Pe < 100). The contrary case is when dispersion is moderate (e.g., Pe > 50) and there is a strongly bimodal distribution of aperture, such that one class of aperture sizes are set apart from the rest. In practice, one would probably never observe breakthrough from a set of apertures that is much smaller than the remaining group. A large set of apertures may lead to fast transport, however, and be observed as a distinct peak in the breakthrough curve.

[20] Note that the individual breakthroughs in Figure 2 have a nearly parabolic shape on this log-log plot but that the total breakthrough is highly skewed toward later time. Such a skewed breakthrough is commonly observed in fractured media and is usually described as breakthrough tailing. The hypothesis that breakthrough tailing is caused by the breakthrough of multiple independent pathways is not new. For example, *Robinson and Tester* [1986] explained breakthrough tailing observed in a fractured formation using multiple pathways. What is different here, is the rationale that total mass and transport rate along all pathways are both related to the mean aperture. This rationale reduces the number of independent parameters necessary to model the breakthrough data.

[21] A power law trend line passing through the peaks of the individual breakthrough curves has a slope of $-3/2$ on a log-log plot (see offset dot-dashed line in Figure 2). This slope is to be expected, because the mass under each curve is proportional to the cube of the aperture, and the offset in time is proportional to the square of the aperture. As concentration is shifted by a power of -3, arrival time is shifted by a factor of 2. The tail slope of the total breakthrough, however, depends upon the shape of the individual breakthrough curves, which is a function of the advective-dispersive model that is chosen. In this example, the commonly used uniform-flow flux-averaged solution of the advection dispersion equation is applied (see Appendix). This particular solution predicts a tail slope of -2 for the total breakthrough (see offset solid line in Figure 2).

[22] The uniform-flow solution of the advection dispersion equation depicted in Figure 2 and the other solutions of the advection-dispersion equation presented in this article are obtained through probabilistic rather than deterministic formulations. The advantage of the probabilistic approach is that it provides sufficient mathematical flexibility such that solutions of the advection-dispersion equation can be accomplished using the same boundary conditions under the assumption of very different test geometries. For example, the radially divergent and convergent solutions both assume an infinite spatial domain, but yield, in the former case, a volume-averaged concentration and, in the latter-case, a flux-averaged concentration (see Appendix). The measured breakthrough curve represents a flux-averaged concentration because concentration is measured in the withdrawn water. Consequently, recovery of tracer is represented here as a first passage time probability solution of the advection-dispersion equation [*Becker and Charbeneau*, 2000]. The injection of a tracer into a formation results in a volume-averaged density of tracer mass. Consequently, injection of tracer is represented here as a probability density solution of the advection-dispersion equation. First passage time solutions for radially convergent tracer experi-

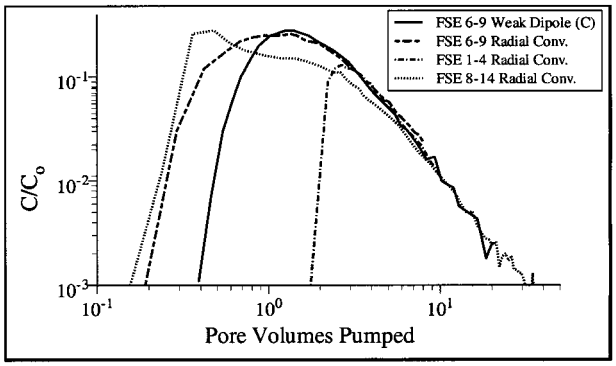

Figure 3. Breakthrough of bromide tracer from several radially convergent and weak dipole tracer experiments among three different well pairs within the FSE well field.

ments been presented previously [*Becker and Charbeneau*, 2000]. An equivalent solution for the push-pull experiment is introduced in the Appendix.

4. Field Experiments

[23] Every summer from 1996 to 2000 forced-gradient tracer experiments were performed in the Forest Service East (FSE) well field at the Mirror Lake Fractured Rock Research Site in Grafton County, New Hampshire (see map by *Becker and Shapiro* [2000], for example). These experiments were of three types: (1) radially convergent, (2) weak-dipole, and (3) single well push pull. In all of these experiments, tracer was injected as a finite volume or "slug" of tracer. In the radially convergent configuration, a well was pumped until approximately steady state heads were achieved. A small volume of tracer-laden water was forced into an isolated interval in another well, some distance away. The volume of injected tracer solution was controlled by deflating and reinflating a packer that sealed the conductive fracture or fractures (see *Shapiro and Hsieh* [1996] for a more detailed description of the injection processes). In the weak-dipole experiments, one well was pumped and approximately 5% of the withdrawn fluid was reinjected at another well 36 m away. Tracer was injected by switching from pumped formation water to a tracer reservoir over a short period of time. Thus the injection of tracer did not alter considerably the flow field during these experiments. After tracer injection was complete, the reinjection of pumped formation water continued. The injection interval was constantly mixed throughout the experiment. Details of the weak-dipole experiments are given by *Becker and Shapiro* [2000].

[24] Push-pull experiments were conducted by injecting a known volume of tracer-laden formation water followed by a "chase" of previously extracted clean formation water. After a known volume of chased water was injected, the well was pumped at the same rate at which tracer had been injected, until approximately 3 times the injected volume had been pumped. Three push-pull experiments were conducted in the summer of 1998, the only difference among the experiments being that different volumes of chase water were used (20, 50, and 60 L). The same tracer injection volume of 2 L was used for all experiments. A number of solute tracers were used in this and other experiments referred to in this article. Bromide, deuterated water, and penta-fluoro-benzonic acid (PFBA) produced almost exactly the same breakthrough in weak-dipole experiments conducted in the FSE well field [*Becker and Shapiro*, 2000]. These tracers will therefore be considered directly comparable conservative tracers for purposes of this article.

[25] The analysis presented here was motivated by the observation that tracer experiments performed under radially convergent or weak-dipole experiment configurations among different well pairs produced similar breakthrough tails. Regardless of transport rate or the free-water diffusion rate of the tracer, these tails all had a power law slope of about -2, when plotted on a normalized plot of log concentration versus log time (Figure 3). The radially convergent and weak-dipole tests therefore suggested that tailing was dominated by advective processes and not matrix diffusion [*Becker and Shapiro*, 2000], and that these advective processes seemed to be acting in a consistent manner within the FSE well field. Push-pull experiments conducted in the FSE well field, however, produced much steeper breakthrough tail power law slopes. The push-pull tests suggested that advection-dominated breakthrough tails may be dependent upon the particular forced-gradient hydraulic configuration chosen. This article offers a conceptual model of transport that appears to explain these observed trends in the data.

5. Interpretation of Tracer Experiments

[26] The conceptual model outlined previously will be used to interpret breakthrough from field experiments conducted at the Mirror Lake Fractured Rock Research Site. Although the same conceptual model will be used, the mathematical formulation must vary with tracer hydraulic configuration. The three configurations to be considered are (1) radially convergent, (2) weak-dipole, and (3) push-pull.

5.1. Radially Convergent Tracer Experiments

[27] Following the previously outlined conceptual model, under an approximately radially convergent test configuration, tracer will move from the injection well to the withdrawal well along independent pathways. Because the volume of injected fluid is expected to be small in comparison to the volume withdrawn, the path lengths will be of approximately similar length. Consequently, the travel time along each path is dictated by velocity along the path, which is proportional to the square of the mean aperture along the path. Mass entering each path is proportional to the cube of the mean aperture along each path. Tracer breakthrough at the withdrawal well is a summation of breakthrough along all of these paths.

[28] Transport along a single pathway may be predicted mathematically using a transfer function. It is assumed here that the transfer functions representing each path are identical, with the exception of their first moment (proportional to the cube of the mean aperture along the path) and second moment (inversely proportional to the square of the mean aperture along each path). Thus the transfer function representing the total breakthrough at the withdrawal well is the result of the summation of multiple transfer functions, shifted in time and scaled according to mass in each pathway.

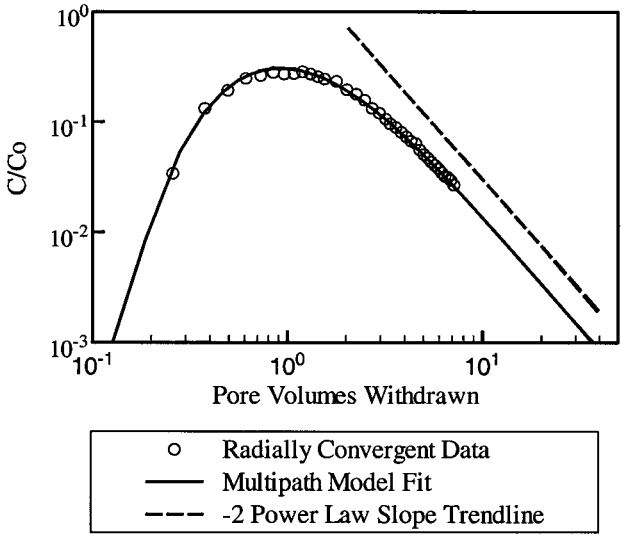

Figure 4. Comparison of the model and bromide breakthrough from a radially convergent tracer experiment conducted between wells FSE 6 and FSE 9 (measured breakthrough also shown in Figure 3).

[29] The transfer function of a single pathway can be expressed as $g(\rho, t)$, where ρ is the ratio of the radial distance from the extraction well to the dispersivity, ($\rho = r/\alpha$) and t is time. It is a simple matter to shift in time the first moment of a transfer function in Laplace space, by taking advantage of the property of Laplace transforms: $f(ct) \leftrightarrow (1/c)\bar{f}(s/c)$, where c is a constant and s is the Laplace parameter. Because the behavior of the composite breakthrough is a function of the relative arrival times of tracer from multiple pathways, it is convenient to express the mean aperture along each pathway with respect to the maximum mean aperture in all channels ($R = H/H_{max}$). In this case, the composite breakthrough resulting from tracer transport through multiple channels described by the transfer function $\bar{g}(\rho, s)$, is expressed in Laplace space as:

$$\bar{g}_m(\rho, s) = \int_{R_{\min}}^{1} \frac{R^3}{R^2}\bar{g}\left(\rho, \frac{s}{R^2}\right)dR, \tag{5}$$

where $\bar{g}_m(\rho, s)$ is the transfer function for multiple pathways and R_{min} is the ratio between the minimum and maximum equivalent aperture paths, $R_{min} = H_{min}/H_{max}$. The mathematical formulation of the transfer function, $\bar{g}(\rho, s)$, used for the radially convergent case is given in Appendix A as equation A8.

[30] The fit of equation 5 to the breakthrough data from the radially convergent experiment conducted between FSE 6 and FSE 9 in 1996 is shown in Figure 4. Model predicted and actual concentrations are normalized as C/C_0, where C and C_0 are the current and initial flux-averaged concentration. Time is normalized as the number of pore volumes withdrawn, or $t/\bar{t}$, where $\bar{t}$ is the mean tracer breakthrough time. The mean tracer breakthrough time, $\bar{t}$, is equal to the first moment of the breakthrough curve or V_f/Q, where V_f is the effective formation volume and Q is the withdrawal rate at the well. The parameter, R, ranges from 1 to 0.01, but the results are not sensitive to the lower range of R because these pathways break through much later than the time of last tracer data point. The model fitting parameters are the effective formation volume, V_f, and the dispersivity, α. For the fit shown in Figure 4 the values of V_f and α are 4.6 m^3 and 6.5 m, respectively. The separation distance between FSE 6 and FSE 9 is 36 m, implying that the total swept volume for this experiment, V_t, is π (36 m)^2 (2 m) = 8100 m^3. The effective porosity for the largest channel transport tracer is therefore $V_f/V_t = 5.6 \cdot 10^{-4}$. For purposes of comparison among tracer tests, it is useful to convert this effective porosity into an effective aperture, by assuming that the wells are connected by a single fracture of constant aperture. Over a 2 m thickness, the aperture of this hypothetical fracture is 1.1 mm. This aperture will be referred to as a "volume equivalent aperture" and used as a conceptual benchmark with which to compare weak dipole and push pull tracer experiments.

5.2. Weak Dipole Tracer Experiments

[31] Four approximately radially convergent (weak-dipole) bromide tracer experiments were conducted at Mirror Lake between FSE 6 (pumping) and FSE 9 (injection) in the summer of 1997, and are documented in detail elsewhere [*Becker and Shapiro*, 2000]. The experiments were identical to one another, except for the pumping and proportional reinjection rate. Only two experiments will be considered here to keep the discussion brief. Experiment B will be discussed because it was conducted at the pumping rate closest to the radially convergent experiment, and experiment C will be discussed because it produced a distinctly different breakthrough than the other three weak-dipole experiments and the radially convergent experiment. Modeling of the experiments is accomplished with the same method applied to the radially convergent experiment except that, for weak-dipole tracer experiments, it is necessary to account for the reinjection of traced fluid at the injection well. In Laplace space, this may be accomplished using the algebraic function [*Becker and Charbeneau*, 2000]:

$$\bar{F}^* = \left[\frac{\bar{F}_S\bar{F}_T}{1 + \varepsilon(1 - \bar{F}_S\bar{F}_T)}\right]. \tag{6}$$

Here $\bar{F}^*$ is the transfer function that accounts for transport in the formation, as well as mixing in the well bore and reinjection. The coefficient, ε, represents the fraction of pumped fluid that is reinjected ($\varepsilon = q/Q$, where Q is the flow rate of net water extracted and q is the flow rate of water reinjected). The source function is the result of mixing and flushing of tracer in the well bore, and was observed to follow an exponentially decaying trend. Application of multiple transfer functions and recycle of transfer functions were addressed by *Becker and Charbeneau* [2000] and will not be repeated here.

[32] Figure 5 shows the model fit to weak-dipole experiment B, where it is assumed that the effective formation volume, V_f, is 5.5 m^3, and the dispersivity is 6.5 m. Experiment B could not be fit using the same model parameters that resulted in a fit of the radially convergent experiment. It was necessary to assume a formation volume

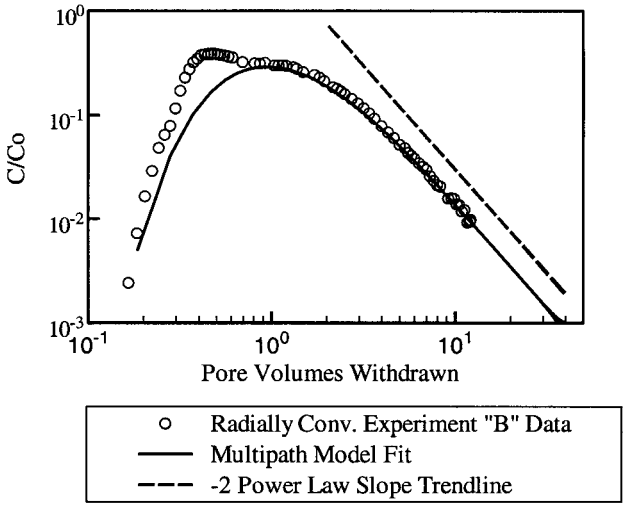

Figure 5. Comparison of the model and bromide breakthrough from weak-dipole tracer experiment "B" conducted between FSE 6 and FSE 9 at a pumping rate of 5.2 L/min.

that was 18% greater than the radially convergent experiment to fit the weak-dipole experiment, although it was not necessary to change dispersivity. The increase in effective formation volume may be due to the divergent flow field around the injection well from constant injection throughout the experiment. This formation volume implies a volume-equivalent aperture of 1.3 mm, which is also 18% greater than that estimated using the radially convergent test.

[33] Note that the data from experiment B is poorly fit by the model at early breakthrough times. An early breakthrough peak that represents about 5% of the injected mass is ignored by this model fit. All of the experiments with higher pumping rates (9.8, 8.3, 5.2 L/min) showed the distinct early peak in breakthrough, whereas the peak was not evident at the lowest pumping rate used (experiment C at 2.9 L/min). To fit the lowest pumping rate, it was necessary to alter the dispersivity parameter in the model but not the effective formation volume. The best fit of the model to experiment C is shown in Figure 6, where V_f, is 5.5 m^3, and the dispersivity is 1.8 m. Thus reducing the pumping rate within a single experiment design results in a decrease in calibrated dispersivity (or increase in Peclet number) of 72 %.

[34] We will not speculate on the cause of the early breakthrough peak so prominent in Figure 5, but to note that *Moreno and Tsang* [1994] have presented numerical experiments that suggest injection in a radially convergent flow field can lead to multiple peak behavior. As discussed previously, the proposed model assumes that the distribution of apertures is somewhat continuous, i.e., that breakthrough from individual channels overlap to some extent. If this early peak represents tracer transport along an anomalously large aperture fracture, a set of model parameters will not properly predict both the peak and the remainder of the breakthrough curve. As a result, we fit only the later time breakthrough in this experiment. Regardless of the cause of the early peak, however, it is clear that dispersivity estimates can be strongly coupled to tracer experiment design. In contrast, the estimate of formation volume derived from the tailing behavior, varied by less than 20% in all weak-dipole and radially convergent experiments.

5.3. Push-Pull Tracer Experiments

[35] Three push-pull tracer experiments were conducted at Mirror Lake in the summer of 1998. All of these experiments were conducted in FSE 9, as this well was the subject of injection for previous weak-dipole and radially convergent tests. Deuterated water and penta-fluoro-benzoic-acid (PFBA) were used as solute tracers. Both solute tracers produced identical breakthrough curves, so only the PFBA data will be presented here.

[36] Breakthrough results from push-pull experiments must be interpreted using a very different mathematical model than that used for the radially convergent and weak-dipole tracer experiments. Because tracer is injected and withdrawn from the same well, tracer mass diverges then converges along approximately the same streamlines. In the absence of hydrodynamic dispersion, one would expect that an instantaneous pulse of tracer injected into a homogeneous and isotropic formation would return an instantaneous pulse of tracer breakthrough. In reality, hydrodynamic dispersion tends to spread out the tracer mass in both the injection and withdrawal phases of the experiment, and its effect is proportional to the transport velocity. Mathematically, this behavior can be considered a radially divergent transport of tracer, followed immediately by a convergent transport of tracer. The mathematical treatment of the push-pull tracer experiment is discussed in Appendix A.

[37] There is inherently less information about transport in a single-well tracer experiment than in a multiple-well tracer experiment because there is no reference length scale. Effective porosity, for example, has no effect on advection of the tracer because divergent and convergent velocities both scale according to porosity. Tracer that goes out fast, comes back fast. In terms of parameter estimation of advection and dispersion, one can no longer fit the mean arrival time, but must fit only the shape of the breakthrough. The shape of the breakthrough is controlled by dispersion,

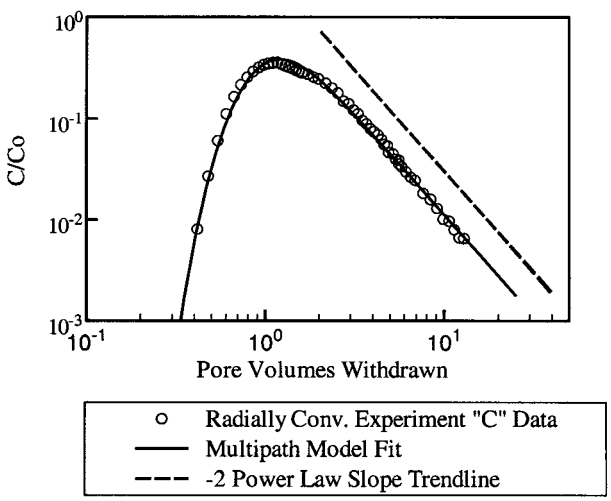

Figure 6. Comparison of the model and bromide breakthrough from weak-dipole tracer experiment "C" conducted between FSE 6 and FSE 9 at a pumping rate of 2.9 L/min.

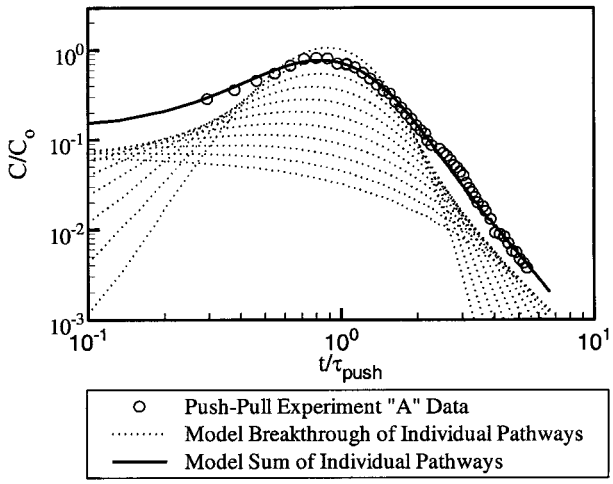

Figure 7. Comparison of the model and PFBA breakthrough from a push-pull experiment conducted in well FSE 9.

which is assumed here to be proportional to average linear velocity. As a consequence, there is no way to decouple the estimation of mean fracture aperture and dispersivity.

[38] An example model run is displayed in Figure 7. The breakthrough that results from injecting all the tracer mass along various pathways is shown as dashed lines. It is clear from these breakthroughs that the shape of the breakthrough depends upon the mean aperture of the pathway. Pathways with small mean apertures (and therefore high velocity) result in very disperse breakthroughs, whereas pathways with larger apertures (and therefore low velocity) result in more condensed breakthroughs. The range in aperture in this simulation is less than an order-of-magnitude, because the smallest apertures affect only the very early and very late time of breakthrough, where actual data are not available. Fit of the model to the data is therefore insensitive to the smallest apertures. The composite of tracer breakthrough along individual paths is also shown in Figure 7. The composite was calculated by multiplying the breakthrough along each pathway by the fraction of mass in that path.

[39] Simulations were performed over a range $0.1 < \tau_{push} < 10{,}000$ to examine the relationship between the push distance and the shape of the breakthrough curve, where

$$\tau_{\text{push}} = \frac{t_{\text{push}}}{\alpha^2}\frac{Q}{2\pi H}, \tag{7}$$

t_{push} is the duration of tracer push, α is dispersivity. The distribution of the breakthrough curve was found to decrease with increasing push (τ_{push}). This trend is a result of the relationship between hydrodynamic dispersion and velocity. When the tracer is pushed a larger distance from the injection well, its velocity slows. Thus, when τ_{push} is large, the mean velocity sampled by the tracer is lower, than when τ_{push} is small. The power law slope of the breakthrough tail increases with increasing τ_{push}. Over the range of τ_{push} tested, the power law slope varied between -2 for the smallest τ_{push} value, and -5.7 for the largest τ_{push} value tested. Values of τ_{push} greater than 10,000 could not be tested as the numerical solution became unstable. A minimum power law slope of -2 is expected, as when tracer is pushed only a short distance away from the injection well, it has little opportunity to disperse. The withdraw phase therefore resembles a radially convergent experiment with a pulse input. As shown previously, a -2 power law slope is expected for the breakthrough tail of radially convergent tracer experiments.

[40] The best fit of the model to Mirror Lake push-pull tracer experiment A is shown in Figure 7. The simulated breakthrough tail has a straight line power law slope of -4.5. The best fit to data was achieved with τ_{push} of approximately 500. Given that the actual t_{push} = 10 min, and assuming that the volume-equivalent fracture aperture from the radially convergent experiment (1.1 mm) is appropriate also for the push-pull experiment, then α is estimated to be 0.08 m or 8 cm. The dispersivity estimated from the push-pull experiment was therefore 80 times smaller than the dispersivity estimated from the radially convergent experiment (6.5 m).

[41] The other two push-pull tracer experiments performed at Mirror Lake were identical to experiment A, with the exception that a greater chase volume was used. Figure 8 displays the results of experiments A, B, and C, where chase volumes of 20, 40, and 60 L of chase water were used, respectively. Accounting for the variation in chase volume is a simple matter of scaling the assumed value of τ_{push} according to these volumes. Figure 8 displays the results of the best fit of the model to experiment A, with τ_{push} = 500, along with the predicted breakthrough when τ_{push} = 1000 and 1500. The scaled result makes a reasonable prediction of the breakthrough in experiment B, mimicking its slightly steeper power law tail slope. The breakthrough of experiment C, however, is not well-predicted by the model, and indeed reverses the trend in increasing power law slope with increasing chase volume.

[42] The reason for this discrepant behavior of experiment C is not clear. The hydraulic response of wells in the FSE well field is correlated over a distances of 10's of meters, resulting in a conceptual model of interconnected high permeability zones, separated by less permeable fracture sets [*Day-Lewis et al.*, 2000]. At a larger injection volume some of the tracer may have migrated to a different hydraulic zone, and therefore exhibited a delayed response upon withdrawal. The duration of experiment C was about 5 hours, which we do not believe is long enough to cause significant drift during injection and withdraw. However, without conducting further experiments with even larger injectate volumes, this explanation is conjecture.

6. Summary

[43] In spite of the fact that a consistent mathematical formulation was used to predict tracer breakthrough under different hydraulic configurations, the transport parameters that resulted in the best fit of model to data varied significantly (Table 1). The model-derived effective formation volume increases slightly from radially convergent to weak dipole configurations, presumably due to the increased flow divergence near the injection well. Effective volume formation cannot be obtained from a single-well push-pull test based on tracer breakthrough alone. The model dispersivity did not vary between radially convergent

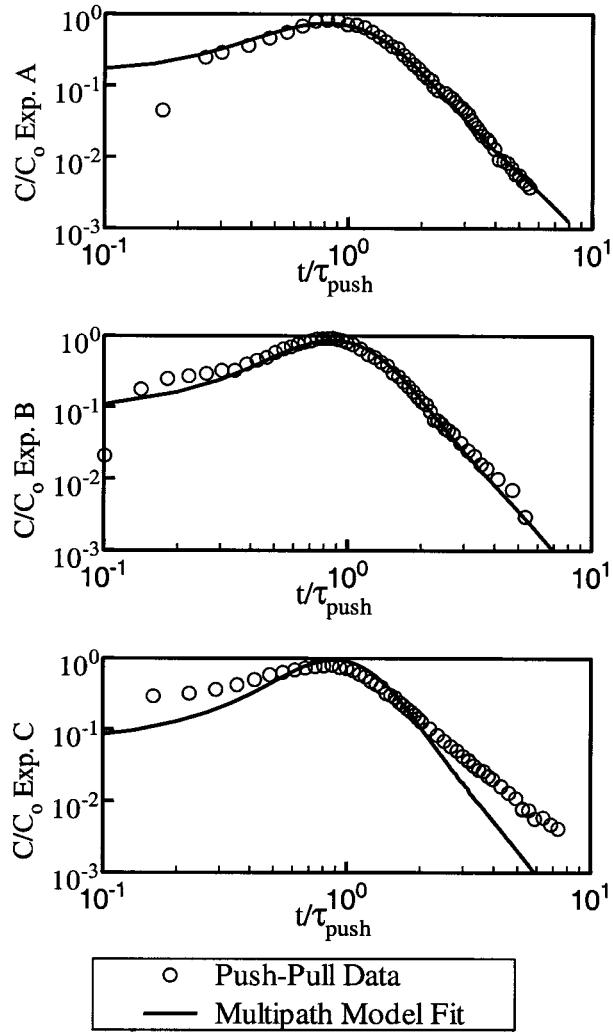

Figure 8. Comparison of the model and PBFA breakthrough among push-pull tracer experiments conducted with varying volumes of chase water (chase volumes 20, 40, and 60 L used in experiments A, B, and C, respectively).

and weak dipole experiments with similar withdrawal rates, but a weak-dipole experiment with a slower withdrawal rate produced a model dispersivity. Model dispersivity cannot be obtained uniquely from the single well test, but if the volume-equivalent aperture derived from the radially convergent test is assumed to be valid for the push-pull test, the implied dispersivity is over an order-of-magnitude smaller than those obtained from the two-well experiments.

7. Conclusions

[44] Radially convergent, weak-dipole, and push-pull tracer experiments were conducted in the FSE well field completed in fractured bedrock near Mirror Lake, New Hampshire. Radially convergent and weak-dipole experiments produced breakthrough tails with a power law slope of -2, regardless of the transport rate or distance. We suggest here that this consistent behavior may have been intrinsic to the forced-gradient tracer experimental design. Our hypothesis is that under a forced gradient water flows through fractures in a highly channelized manner. In accordance with the cubic law tracer mass is distributed to each channel in proportion to the cube of the mean aperture, and migrates at a rate in proportion to the square of the mean aperture. Based upon this hypothesis, mathematical "multichannel" transport models for radially convergent, weak-dipole, and push pull tracer tests were developed. The theoretical models predict the -2 power law slope observed in radially convergent and weak-dipole experiments, and the steeper slopes observed in push-pull experiments conducted in the same formation. Power law slopes on tracer breakthrough tails are predicted by the models in the absence of matrix diffusion.

[45] The fact that late-time breakthrough is dependent upon the tracer experiment design has important implications for the measurement of transport parameters in fractured media. For purposes of this article, we considered three processes of mass spreading that influence breakthrough tailing: (1) hydrodynamic dispersion, a local mixing phenomenon that increases always in the direction of flow, (2) heterogeneous advection, which results from the separation of mass in different flow channels and may be partially reversible when the flow field is reversed, and (3) matrix diffusion which describes mass exchange between fractures and the surrounding rock. Previous tracer experiments in this formation have determined that (3) does not have a significant impact on the breakthrough tail at the time-scale of these tracer tests [*Becker and Shapiro*, 2000]. One might expect therefore that if (2) is properly described by the multichannel approach, then (1) should be correctly modeled with the advection-dispersion equation. In other words, if we remove the effect of large scale mixing caused by imposed flow field then we should be able to consistently measure local hydrodynamic dispersivity independent of tracer test configuration.

[46] We were apparently unable to separate the effects of hydrodynamic dispersion and heterogeneous advection with the multichannel model. Although the model provided excellent fits to all but one of the datasets, transport parameters derived from these models were inconsistent. Multichannel interpretations of the radially convergent and weak-dipole experiments provided an estimate of effective formation volume that varied only by 16%, whereas dispersivity estimates varied over 260%. Formation volume cannot be obtained from single-well push-pull experiments because there is no reference length scale. Assuming that the fracture aperture derived from the radially convergent experiment is correct, however, we obtained an estimate of

Table 1. Comparison of Model Transport Parameters for Various Tracer Experiment Configurations[a]

Tracer Experiment	V_f, m	Effective Porosity	$H_{vol\ equiv}$, (mm)	α, m
Rad. convergent	4.6	5.6×10^{-4}	1.1	6.5
Weak dipole B	5.5	6.8×10^{-4}	1.3	6.5
Weak dipole C	5.5	6.8×10^{-4}	1.3	1.8
Push-pull A	NA	NA	NA	0.08[b]

[a]Two well experiments were conducted over a distance of 36 m, and the total effective formation volume (V_t) is assumed to be 8100 m^3. NA means that effective volume formation, V_f, cannot be estimated from a push-pull experiment.

[b]Value for dispersivity obtained by assuming volume equivalent aperture derived from radially convergent test.

dispersivity from models of the push-pull experiments. The modeled dispersivity from the push-pull experiments was 80 times smaller than that obtained from the radially convergent experiment.

[47] Although advection can explain the power law slope observed in the breakthrough curves, therefore, we cannot entirely discount the relationship between hydrodynamic dispersion and the imposed flow field. There may be a continuum between hydrodynamic dispersion and heterogeneous advection. In any case, these results tend to undermine the argument that conducting tracer experiments in a push-pull configuration removes the effect of hydrodynamic dispersion and heterogeneous advection from the breakthrough tail. Push-pull experiments do not necessarily produce a breakthrough tail characteristic of matrix diffusion.

[48] Our interpretation of these experiments is that it is possible to obtain very different estimates of transport parameters under different tracer experiment configurations, possibly due to sample bias caused by introduction of artificial tracer into the formation. If our analysis is correct, then there is potential for similar ambiguity from tracer experiments conducted in any highly heterogeneous geologic medium. The obvious way to determine whether a unique set of transport parameters is being measured from a forced gradient tracer experiment, is to repeat tracer experiments under different forced-gradient configurations. Unfortunately, if conflicting estimates of transport parameters are obtained, there is no clear way to decide which estimate, if any, is correct. It would seem that greater efforts should be made to compare artificial and natural tracer transport, to determine the relevance of forced gradient tracer experiments to real-world problems.

Appendix A: A First Passage Time Push-Pull Solution

[49] The radially convergent solution presented in the text is based upon a probabilistic model of transport. It considers tracer injection to be equivalent to a probability density function of tracer mass, and withdrawal to be equivalent to a probability density function of first passage times of tracer transport from injection to recovery. The essence of the method is to assume that the probability density of probabilistic ''particles'' is equivalent to a volume-averaged concentration [*Becker and Charbeneau*, 2000]. Likewise, probability flux out of a domain (probability density of first passage times) is equivalent to a flux-averaged concentration. Once the equivalence between probability and concentration is assumed, one may solve either the Fokker-Planck probability equation, or the advection-dispersion equation to the same result.

[50] The advection-dispersion equation can be expressed in radial coordinates as [*Moench and Ogata*, 1981]:

$$\frac{\partial C}{\partial \tau} = \frac{1}{\rho}\frac{\partial C}{\partial \rho} + \frac{1}{\rho}\frac{\partial^2 C}{\partial \rho^2}, \tag{A1}$$

where

$$\tau = \frac{tA}{\alpha^2}, \rho = \frac{r}{\alpha}, C = \frac{C_V}{C_0}. \tag{A2}$$

[51] Here, α is the dispersivity, C_V is the volume averaged concentration, and C_0 is the initial volume-averaged concentration. The parameter, A, accounts for the radial geometry of the flow in either a porous or fractured medium. For example, in a well pumping at a rate, Q, in a single fracture of mean aperture, H, this parameter is defined as:

$$A = \frac{Q}{2\pi H}. \tag{A3}$$

[52] Equation A1 is conveniently solved in Laplace space, so A1 is rewritten in Laplace space with the overbar representing transformed variables, and s, is the Laplace variable.

$$s\overline{C} = \frac{1}{\rho}\frac{\partial \overline{C}}{\partial \rho} + \frac{1}{\rho}\frac{\partial^2 \overline{C}}{\partial \rho^2}, \tag{A4}$$

[53] Divergent advective-dispersive transport of tracer away from an injection well can be considered mathematically equivalent to the probability of a particle starting at the outer radius of an injection well, being found at a some radial position away from the center of the well, at a given time. A continuous injection of tracer is represented by a continuous introduction of probabilistic particles, and results in a cumulative probability density away from the well. Injection of an instantaneous pulse of mass (represented by a Dirac Delta Function) is represented by an introduction of a single probabilistic particle, and results in a probability density function. *Moench and Ogata* [1981] solved the continuous injection case by assuming that the concentration at the injection well was constant, and the concentration approached zero an infinite distance away from the well. Their solution in Laplace space may be expressed as:

$$s\overline{C} = \frac{1}{s}\exp\left(\frac{\rho - \rho_w}{2}\right)\frac{Ai[y(\rho, s)]}{Ai[y(\rho_w, s)]}, \tag{A5}$$

where,

$$y(\rho, s) = \left(s\rho + \frac{1}{4}\right)s^{-2/3}, \tag{A6}$$

and Ai( ) is the Airy Function. As equation A5 is equivalent to a probability density function, we can consider the left-hand-side of this equation to be the cumulative probability density function, $\bar{P}(\rho, s)$. We obtain the probability density function, $\bar{p}(\rho, s)$ by taking the time derivative of the cumulative density function:

$$\bar{p}(\rho, s) = \frac{1}{s}\exp\left(\frac{\rho - \rho_w}{2}\right)\frac{Ai[y(\rho, s)] + 2s^{1/3}Ai'[y(\rho, s)]}{2Ai[y(\rho_w, s)]}, \tag{A7}$$

where Ai′( ) is the derivative of the Airy Function.

[54] Each point in the probability density function, $\bar{p}(\rho, s)$ may be considered a Dirac source unto itself. The arrival at the well can therefore be considered the summation of the first passage times from all particles resulting from the probability density function, determined at the time of cessation of push, and beginning of pull (it is assumed that

there is no rest period in between and that flow is steady during push and pull stages). The radially convergent first passage time function in Laplace space is [*Becker and Charbeneau*, 2000]:

$$\bar{g}(\rho, s) = \exp\left(\frac{\rho - \rho_w}{2}\right) \frac{Ai[y(\rho, s)]}{Ai[y(\rho_w, s)]} \tag{A8}$$

[55] The push-pull breakthrough was calculated by first solving the divergent function, $\bar{p}(\rho, s)$ at a many ρ values, at the time corresponding to the duration of the push phase:

$$\bar{g}_{pp}(s) = \int_{\rho_{\min}}^{\rho_{\max}} \bar{p}(\rho, s)|_{\tau_{push}} \bar{g}(\rho, s) d\rho, \tag{A9}$$

where $\bar{p}(\rho, s)|_{\tau push}$ is the push or divergent function evaluated at the maximum time of the push phase, τ_{push}, $\bar{g}(\rho, s)$ is the radially convergent breakthrough evaluated at a radial distance from the injection well, ρ, and ρ_{min} and ρ_{max} represent the range of distance away from the well that the tracer is assumed to be pushed. Mathematically, tracer is predicted to be pushed an infinite distance from the injection well. In practice, $\rho_{\max}$ was determined by finding where the normalized concentration of tracer, C/C_o fell below 10^{-6}.

[56] Equation A9 was approximated by calculating the divergent or push function at the maximum time of the push phase, inverting the solution to the time domain, then using each concentration point along that function as a source for the convergent solution. The breakthrough for the pull phase was calculated by summing the radially convergent transport from 100 points along the push function. Increasing the number of points did not affect the solution, so 100 points was considered sufficient. Summation of the convergent function, $\bar{g}(\rho, s)$ for all values of ρ, was accomplished in Laplace space, as the function was better behaved in Laplace than Time space. The Laplace inversion algorithm used is based upon a Fast-Fourier Transform (FFT), which provided the sufficient speed of inversion necessary to perform repeated calculations for multiple pathways. Numerical calculation was carried out using a Fortran program that employs the FFT algorithm from *Numerical Recipes* [*Press et al.*, 1999]. This solution was found to closely agree with the solution of *Haggerty and Fleming* [1999], except where dispersivity was very large (Peclet numbers less than about 5). The difference in the two solutions is attributed to the closed inlet condition imposed by *Haggerty and Fleming* [1999].

[57] The above solution is for a single path in the multipath model. The solution must be recalculated for each of the assumed pathways, with varying equivalent aperture. As in the radially convergent model, different mean aperture values lead to a different values of the parameter, A. Likewise, each aperture leads to a different value of Q attributed to that pathway. Multiple paths were simulated by varying A in proportion to the square of the ratio of the aperture of any given path to the value of the maximum aperture of all paths, $H_{\max}$:

$$A = A_{\max} \frac{H^2}{H_{\max}^2} = A_{\max} R^2, \tag{A10}$$

where

$$R = \frac{H}{H_{\max}}.$$

Because time is normalized to the value of A, it is only the relative value of A that is significant in the model.

[58] Varying the value of A in the model is equivalent to shifting the breakthrough curve along in time. This is conveniently accomplished in Laplace space by taking advantage of the property of Laplace transforms: $f(ct) \leftrightarrow (1/c)\bar{f}(s/c)$, where c is a constant and s is the Laplace parameter. The composite breakthrough at the well during the pull phase is the result of summing all pathways of different aperture:

$$\bar{g}_{pp}(\rho, s') = \int_{R_{\min}}^{1} \frac{R^3}{R^2} \bar{g}_{pp}\left(\rho, \frac{s}{R^2}\right) dR \tag{A11}$$

where s' is the shifted Laplace parameter, and $R_{\min}$ is the ratio between the minimum and maximum equivalent aperture paths. This is the same procedure followed for the radially convergent multipath solution (equation A8). Equation A11 was approximated by summing the results of a finite number of pathways. Good solutions could be obtained by using only about 10 pathways. Run time calculations on a Sun Ultra 5 workstation was about 15 seconds for most runs.

[59] **Acknowledgments.** These investigations were conducted with the support of the Toxic Substances Hydrology and National Research Programs administered by the U. S. Geological Survey and the National Research Council Post-Doctoral Associateship Program. The authors gratefully acknowledge field and laboratory support by Paul Hsieh, Rick Perkins, Carole Johnson, and John Jaacks, and the logistical support provided by Mr. C. Wayne Martin of the U.S. Forest Service. The Hubbard Brook Experimental Forest is operated and maintained by the Northeastern Forest Experiment Station, USDA Forest Service, Radnor, Pennsylvania. We appreciate the thoughtful reviews provided by Allen Moench, Paul Hsieh, and the anonymous reviewers for Water Resources Research. This article benefited greatly from the comments of Paul Reimus of Los Alamos Laboratory.

References

Abelin, H., L. Birgersson, L. Moreno, H. Widen, T. Agren, and I. Neretnieks, A large-scale flow and tracer experiment in granite, 2, Results and interpretation, *Water Resour. Res.*, *27*(12), 3119–3135, 1991.

Becker, M. W., Tracer tests in a fractured rock and their first passage time mathematical models, Ph.D. thesis, Univ. of Texas at Austin, Austin, 1996.

Becker, M. W., and R. J. Charbeneau, First-passage-time transfer functions for groundwater tracer tests conducted in radially convergent flow, *J. Contam. Hydrol.*, *45*(4), 361–372, 2000.

Becker, M. W., and A. M. Shapiro, Tracer transport in fractured crystalline rock: Evidence of nondiffusive breakthrough tailing, *Water Resour. Res.*, *36*(7), 1677–1686, 2000.

Bourke, P. J., Channeling of flow through fractures in rock, in *GEOVAL-87 International Symposium*, Swed. Nucl. Power Insp. (SKI), Stockholm, 1987.

Callahan, T. J., P. W. Reimus, R. S. Bowman, and M. J. Haga, Using multiple experimental methods to determine fracture/matrix interactions and dispersion of nonreactive solutes in saturated volcanic tuff, *Water Resour. Res.*, *36*(12), 3547–3558, 2000.

Chao, H.-C., H. Rajaram, and T. Illangasekare, Intermediate-scale experiments and numerical simulations of transport under radial flow in a two-dimensional heterogeneous porous medium, *Water Resour. Res.*, *36*(10), 2869–2884, 2000.

Day-Lewis, F. D., P. A. Hsieh, and S. M. Gorelick, Identifying fracture-zone geometry using simulated annealing and hydraulic-connection data, *Water Resour. Res.*, *36*(7), 1707–1721, 2000.

Frost, L. H., N. W. Scheier, and C. C. Davison, Transport properties in highly fractured rock experiment—Phase 2 tracer tests in fracture zone 2, 65 pp., At. Energy of Can. Ltd., Mississauga, Ontario, 1995.

Guimera, J., and J. Carrera, A comparison of hydraulic and transport parameters measured in low-permeability fractured media, *J. Contam. Hydrol.*, *41*(3–4), 261–281, 2000.

Haggerty, R. and S. W. Fleming, STAMMT-R: Solute Transport and Multirate Mass Transfer in Radial Coordinates, version 1.01, 58 pp., Sandia Natl. Lab., Albuquerque, N.M., 1999.

Haggerty, R., and S. M. Gorelick, Design of multiple contaminant remediations: Sensitivity to rate-limited mass transfer, *Water Resour. Res.*, *30*(2), 435–446, 1994.

Haggerty, R., and S. M. Gorelick, Multiple-rate mass transfer for modeling diffusion and surface reactions in media with pore-scale heterogeneity, *Water Resour. Res.*, *31*(10), 2383–2400, 1995.

Haggerty, R., S. A. McKenna, and L. C. Meigs, On the late-time behavior of tracer test breakthrough curves, *Water Resour. Res.*, *36*(12), 3467–3479, 2000.

Hakemi, E., and E. Larsson, Aperture measurements and flow experiments on a single natural fracture, *Int. J. Rock Mech. Min. Sci Geomech. Abstr.*, *33*(4), 395–404, 1996.

Indelman, P., and G. Dagan, Solute transport in divergent radial flow through heterogeneous porous media, *J. Fluid Mech.*, *384*, 159–182, 1999.

Jardine, P. M., W. E. Sanford, J. P. Gwo, O. C. Reedy, D. S. Hicks, J. S. Riggs, and W. B. Bailey, Quantifying diffusive mass transfer in fractured shale bedrock, *Water Resour. Res.*, *35*(7), 2015–2030, 1999.

Karasaki, K., B. Freifeld, A. Cohen, K. Grossenbacher, P. Cook, and D. Vasco, A multidisciplinary fractured rock characterization study at Raymond field site, Raymond, CA, *J. Hydrol.*, *236*(1–2), 17–34, 2000.

Moench, A. F., Convergent radial dispersion in a double-porosity aquifer with fracture skin: Analytical solution and application to a field experiment in a field experiment in fractured chalk, *Water Resour. Res.*, *31*(8), 1823–1835, 1995.

Moench, A. F., and A. Ogata, A numerical inversion of the Laplace transform solution to radial dispersion in a porous medium, *Water Resour. Res.*, *17*(1), 250–252, 1981.

Moreno, L., and C. F. Tsang, Multiple-peak response to tracer injection tests in single fractures: A numerical study, *Water Resour. Res.*, *27*(8), 2143–2150, 1991.

Moreno, L., and C.-F. Tsang, Flow channeling in strongly heterogeneous porous media: A numerical study, *Water Resour. Res.*, *30*(5), 1421–1430, 1994.

National Research Council, *Rock Fractures and Fluid Flow: Contemporary Understanding and Applications*, Natl. Acad. Press, Washington, D. C., 1996.

Neretnieks, I., Diffusion in the rock matrix: An important factor in radionuclide retardation?, *J. Geophys. Res.*, *85*, 4379–4397, 1980.

Neuzil, C. E., and J. V. Tracy, Flow through fractures, *Water Resour. Res.*, *17*(1), 191–199, 1981.

Oron, A. P., and B. Berkowitz, Flow in rock fractures: The local cubic law assumption reexamined, *Water Resour. Res.*, *34*(11), 2811–2825, 1998.

Ostensen, R. W., Tracer tests and contaminant transport rates in dual-porosity formations with application to the WIPP, *J. Hydrol.*, *204*(1–4), 197–216, 1998.

Parney, R., and L. Smith, Fluid velocity and path length in fractured media, *Geophys. Res. Lett.*, *22*(11), 1437–1440, 1995.

Press, W. H., S. A. Teukolsky, W. T. Vetterling, and B. P. Flannery, *Numerical Recipes in Fortran 77: The Art of Scientific Computing*, 1486 pp., Cambridge Univ. Press, New York, 1999.

Rasmuson, A., and I. Neretnieks, Radionuclide transport in fast channels in crystalline rock, *Water Resour. Res.*, *22*(8), 1247–1256, 1986.

Raven, K. G., K. S. Novakowski, and P. A. Lapcevic, Interpretation of field tracer tests of a single fracture using a transient solute storage model, *Water Resour. Res.*, *24*(12), 2019–2032, 1988.

Reimus, P. W., A. Adams, M. J. Haga, A. Humphrey, T. Callahan, I. Anghel, and D. Counce, Results and interpretation of hydraulic and tracer testing in the Prow Pass Tuff at the C-Holes, Yucca Mountain Site Characterization Project Milestone, *Rep. SP32E7M4*, Los Alamos Natl. Lab., Los Alamos, N. M., 1999.

Robinson, B., and J. Tester, Characterization of flow maldistribution using inlet-outlet tracer techniques: An application of internal residence time distributions, *Chem. Eng. Sci.*, *41*(3), 469–483, 1986.

Shapiro, A. M. and P. A. Hsieh, A new method of performing controlled injection of traced fluid in fractured crystalline rock, in *U.S. Geological Survey Toxic Substances Hydrology Program Technical Meeting*, edited by D. W. Morganwalp and D. A. Aronson, pp. 131–136, U.S. Geol. Surv., Colorado Springs, Colo., 1996.

Shapiro, A. M., and J. R. Nicholas, Assessing the validity of the channel model of fracture aperture under field conditions, *Water Resour. Res.*, *25*(5), 817–828, 1989.

Tsang, C.-F., and I. Neretnieks, Flow channeling in heterogeneous fractured rocks, *Rev. Geophys.*, *36*(2), 275–298, 1998.

Tsang, C. F., Y. W. Tsang, and F. V. Hale, Tracer transport in fractures: Analysis of field data based on a variable-aperture channel model, *Water Resour. Res.*, *27*(12), 3095–3106, 1991.

Tsang, Y. W., Usage of "equivalent apertures" for rock fractures as derived from hydraulic and tracer tests, *Water Resour. Res.*, *28*(5), 1451–1455, 1992.

M. W. Becker, Department of Geology, State University of New York at Buffalo, Buffalo, NY 14260, USA. (mwbecker@geology.buffalo.edu)

A. M. Shapiro, Water Resources Division, U.S. Geological Survey, Reston, VA 20192, USA.